

Short Communication

Corrosion Behavior of L415 Natural Gas Pipeline in High pressure Oxygen-enriched and High salt Environment

Hailing Li^{1,2}, Hongxia Wan¹, Zhiyong Liu^{1,*}, Cuiwei Du^{1,*}, Yuning Liu¹, Xiaogang Li¹

¹ Institute for Advanced Materials and Technology, University of Science and Technology Beijing, Beijing 100083, China

² College of Materials Science and Engineering, Hebei University of Engineering, Handan 056038, Hebei, China

*E-mail: liuzhiyong7804@126.com, dcw@ustb.edu.cn

Received: 22 April 2017 / Accepted: 7 June 2017 / Published: 12 July 2017

The corrosion behavior of L415 steel natural gas pipeline under high pressure oxygen-rich and high-salt environment was investigated by combining electrochemistry and immersion test with scanning electron microscope and X-ray diffraction. Results show that serious corrosion of L415 steel occurred in high-pressure oxygen-rich and high-salt environment with corrosion rate of 0.847 mm. a-1, which belonged to serious corrosion level. The ions of the leaching liquid and the oxygen-rich environment can promote L415 steel corrosion. In terms of morphology, a thick layer of corrosion products was generated from the pitting of L415 steel surface, and some area even had a severe corrosion groove after removal of corrosion products. The corrosion of L415 steel was quite severe in high-pressure oxygen-rich and high salt environment, that the steel must be kept in inert atmosphere and swept with water having low salt concentration.

Keywords: L415 steel High pressure oxygen-enriched and high salt environment Corrosion behavior

1. INTRODUCTION

With the development of oil and natural gas industry, pipeline are lay to transport oil and natural gas resources, and a huge sum of money is invested on the laying of pipelines around the world. The service life of a pipeline has gradually become one of the key factors in the development of oil and gas resources [1-4]. However, the corrosion failure of oil and gas pipeline has frequently led to major accidents, which cause severe economic losses and social consequences [5-7]. Corrosion is one of the main factors that threaten the safety and the service life of a pipeline. In 1998, Stanley [8] analyzed the accident statistics of the pipeline failure, with about 51% failure being related to

corrosion. Crabtree [9] analyzed tubing failure between 1997 and 2007, and their statistics found that corrosion caused 33% of the pipeline failure.

Oxygen and salt environment can lead to steel corrosion [10-12]. Corrosion of L415 steel occurs in high pressure oxygen-rich and high salt environment, which considerably accelerated the corrosion inside the pipeline, especially pitting corrosion[13]. Pitting corrosion is one of the major causes of crack initiation [14, 15]. Pitting does not only generate high stress concentration effects that promote crack initiation and propagation, but also promote some corrosive substances such as Cl^- enrichment in corrosion pits that result in interior acidification of the pitting corrosion solution. These factors cause the rapid electrochemical dissolution of the matrix in the crack tip position and then the crack extension [16-18]. Hence, the pitting corrosion would cause stress corrosion and severe harm to the pipeline service security.

In this work, the corrosion behavior of L415 pipeline was studied in the laboratory under simulated conditions of leaching liquid. The technology of electrochemical polarization, electrochemical impedance spectroscopy and immersion test, combined with SEM and XRD, were used to investigate the occurrence of pitting corrosion on an L415 carbon steel pipeline. These tests provide a basis for reducing corrosion in engineering, confirm high-pressure oxygen-rich and high salt environment as reasons behind severe corrosion, allow a better understand of the pitting behavior, and establish the basis of relevant protective measures.

2. EXPERIMENTAL

2.1 The research background

The buried L415 steel pipeline of natural was around 100 km long, with specifications of $\Phi 508 \times 7.1$. As showed in Fig.1, Fig1 (a₁) is the exterior morphology of L415 pipeline, and Fig1 (a₂) is the internal morphology with much visible pitting. The entire surface of the L415 pipeline steel suffers from severe corrosion with many pitting holes (Fig1b) shown in stereoscopic microscope. According to on-site construction records, the pressure test, sweeping water, and packing work were completed after the pipeline were accomplished in July 2012. The pressure medium was air at 4.5 MPa, with perforation occurring after 7-12 months. The perforation rate was as high as 1.4 mm/a; this phenomenon was rare in corrosion cases. To determine the reason behind pitting corrosion, the behavior and mechanism of L415 steel was studied in simulated high-pressure, oxygen-rich and high salt environment.

2.2 Materials

All samples in the experiment were cut from the same piece of buried L415 steel pipeline for natural gas, Table 1 list the chemical compositions of the pipeline.

2.3 Test condition

The test solution was a leaching liquid, which came from rust layer after holding the pressure for about 7-12 months in the liquid phase environment. Through chemical analysis, the ions in leaching liquid from rust layer (mg/L) are Na^+ 469.182, K^+ 28.846, Mg^{2+} 16.842, Ca^{2+} 37.756, F^- 7.135, Cl^- 54.890, SO_4^{2-} 204.015, NO_3^- 4.716. Following the law of mass conservation and charge conservation of cationic and anionic ion, a high concentration instead of low concentration is adopted when a completely match cannot be obtained, and the common chemical reagent is used to confect the simulated solution. Following these principles, the simulated solution for leaching liquid (g/L) is NaF 0.0157, CaCl_2 0.0888, KNO_3 0.091, NaHCO_3 0.294, Na_2SO_4 0.213, $\text{MgSO}_4 \cdot 7\text{H}_2\text{O}$ 0.172 and the pH is 4.5 adjusting with dilute hydrochloric acid solution. The pitting corrosion of L415 steel was studied in various leaching liquid irons, the specific components were showed in solution 1, 2 and 3 in Table 2, respectively. All solution were prepared from analytical grade reagents in deionized water.

Table 2. Components of various leaching liquid irons (Solution 1, 2, 3)

	NaF	CaCl_2	KNO_3	NaHCO_3	Na_2SO_4	$\text{MgSO}_4 \cdot 7\text{H}_2\text{O}$
Solution 1	0.0157	0.0888	0.091	0.294	0.213	0.172
Solution 2	0.0314	0.1776	0.182	0.588	0.426	0.344
Solution 3	0.157	0.888	0.91	2.94	2.13	1.72

2.4 Electrochemical measurement

The size of electrochemical specimens was 10mm×10mm×3mm, all the electrochemical specimens were coated with an epoxy resin, leaving an exposure area of 10 mm×10 mm as a working electrochemical, which was ground sequentially to 2000 grit emery paper, and cleaned using acetone. The samples were vertical suspend in the autoclave with solution 1 and 2 at 5MPa and maintained under constant pressure with 99.99% N_2 and air (80% N_2 -20% O_2). Electrochemical tests were conducted with a three-electrode cell system on a PARSTAT2273 electrochemical workstation. The specimen was the working electrode, Ag/AgCl was the reference electrode, and a platinum plate was the counter electrode. Prior to measurement, the specimens were treated with the leaching liquid solution for 30 min to ensure steady corrosion potential. Electrochemical tests included EIS and potentiodynamic polarization curves. The EIS was tested at the disturbance of 10 mV AC voltage and at the frequency ranged of 100 KHz to 10 mHz. Potentiodynamic polarization curves were tested at a potential sweeping rate of 0.5 mV/s, and the scanning voltage range was relatively open circuit potential from -0.5 V (vs. SCE) to 1 V (vs. SCE).

2.5 Immersion test

Table 1. Chemical composition (wt.%) of L415 pipeline steel

Element	C	Si	Mn	P	S	Nb	Ni	Cr	Mo	Cu	Fe
L415	0.1	0.22	1.22	0.012	0.0033	0.028	0.032	≤0.01	≤0.01	≤0.01	balance

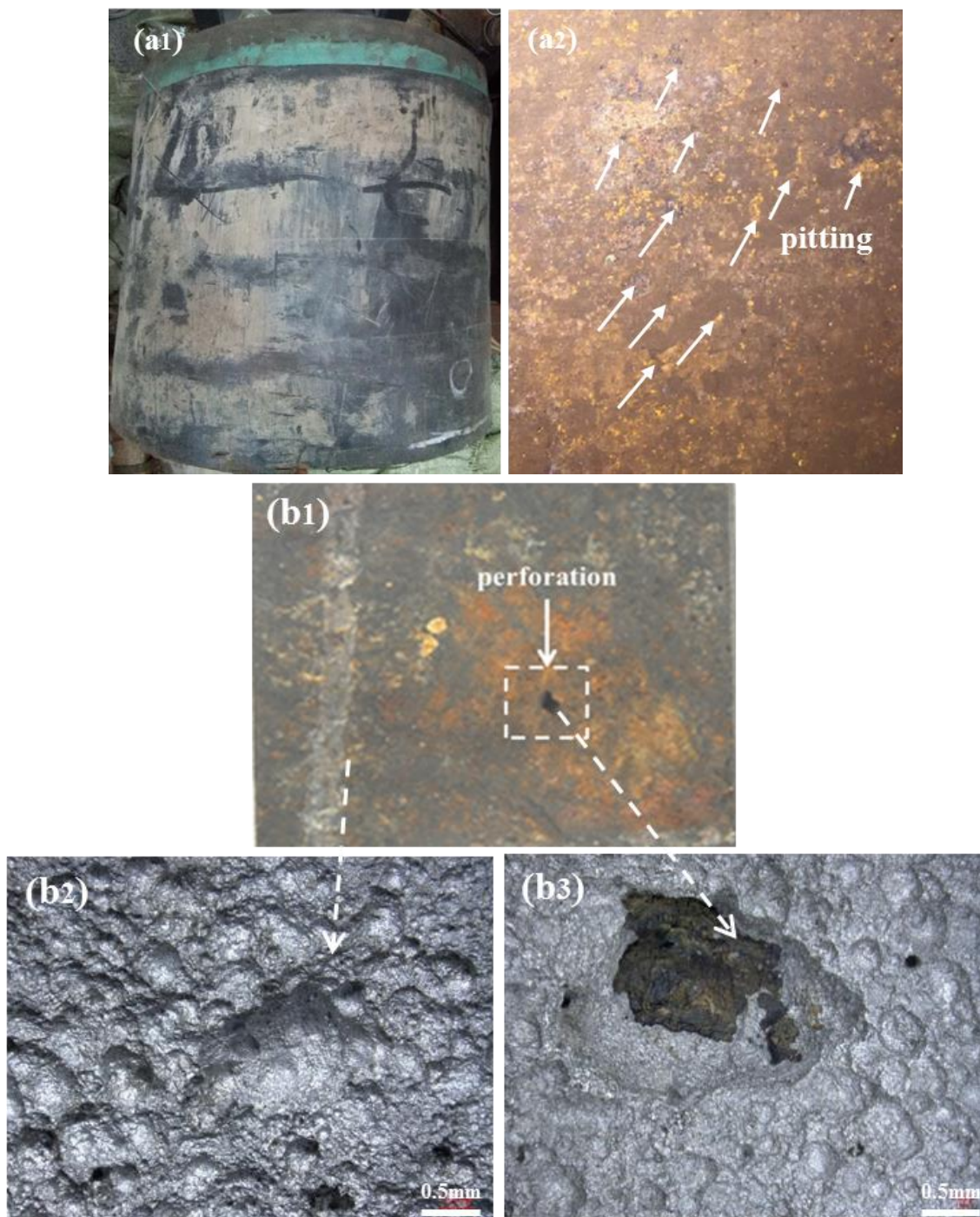


Figure 1. Corrosion perforation morphology of L415 pipeline (a) macro-morphology and (b) Stereoscopic morphology

The size of immersion samples was 35mm×25mm×2mm. Sample surfaces were burnished to 1500 grits and cleaned in distilled water and acetone. Three parallel samples were used in each experimental condition. The samples were vertical suspend in the autoclave with solution 1, 2 and 3 in 5MPa high-pressure with air (80%N₂-20%O₂). Pictures were taken with a camera before and after experiment. After immersing for 90 days, some corrosion products were scraped down from the samples to analysis the composition by XRD; Other corrosion products were thoroughly removed using a descaling solution containing 500 mL HCl (ρ=1.189), 500 mL distilled water and 3.5g hexamethylenetetramine. After rinsing and drying, the specimen morphology was observed with stereoscopic microscope and scanning electron microscopy (SEM; Quanta 250).

All the experiments were conducted at room temperature(~22°C).

3. RESULTS and DISCUSSION

3.1 Electrochemical measurements

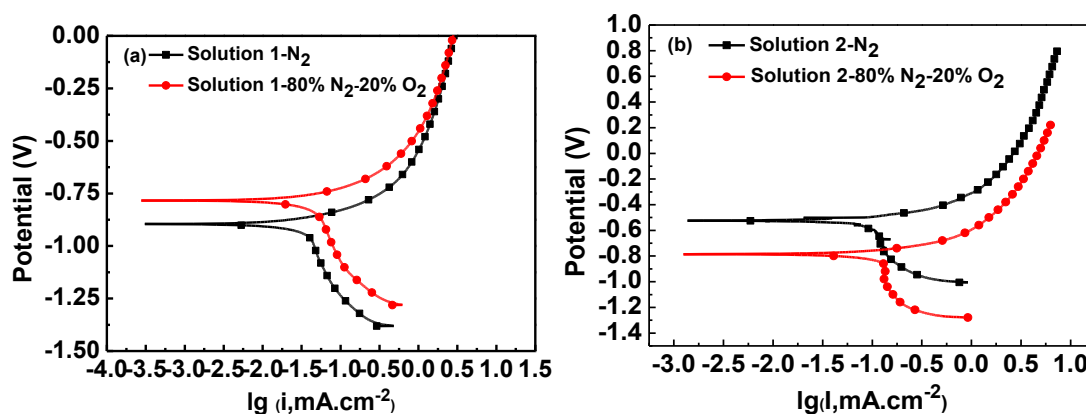


Figure 2. Polarization curves of L415 pipeline steel obtained in solution 1 and solution 2 with 99.99% N₂ and 80%N₂-20%O₂

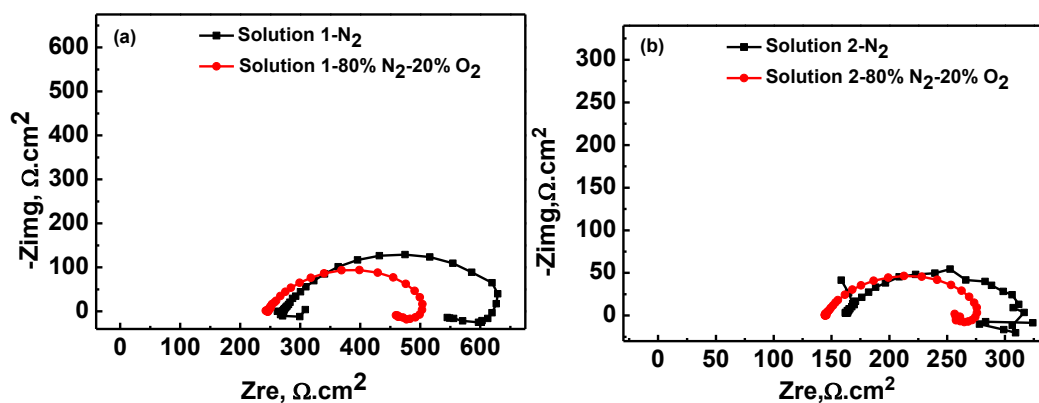


Figure 3. EIS of L415 pipeline steel under various irons in solution 1 and solution 2 with 99.99% N₂ and 80%N₂-20%O₂

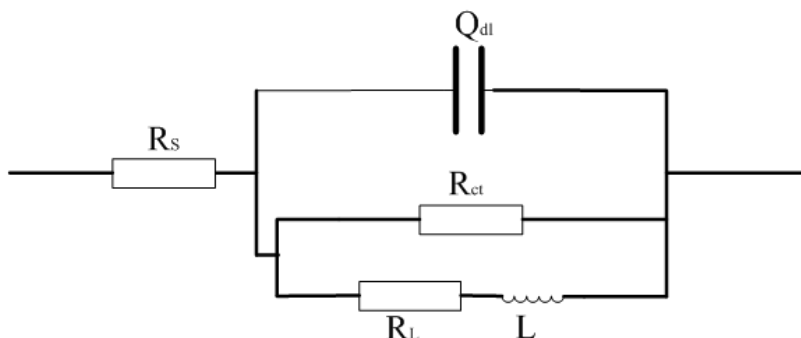


Figure 4. Equivalent EIS circuit of the L415 pipeline steel

Table 3. Corrosion potential and corrosion current density of L415 pipeline steel in simulated leaching liquid environment

	Solution1- 99.99% N ₂	Solution 1- 80% N ₂ -20% O ₂	Solution 2- 99.99% N ₂	Solution 2- 80% N ₂ -20% O ₂
E _{corr} /V	-0.896	-0.795	-0.525	-0.784
I _{corr} /mA.cm ⁻²	0.031	0.043	0.061	0.054

Table 4. EIS fitting results of L415 pipeline steel from the equivalent circuit

Component parameter	Solution1- 99.99% N ₂	Solution1- 80% N ₂ -20% O ₂	Solution2- 99.99% N ₂	Solution2- 80% N ₂ -20% O ₂
R _{ct}	281.4	216.7	94.43	110.4
R _L	96.43	61.86	55.14	28.24

Fig.2 shows the polarization curves of L415 pipeline steel in simulated leaching liquid environments. Active and diffusion corrosion controlled the anode and cathode polarizations, respectively. Table 3 shows the values of corrosion potential and corrosion current density after fitting. Corrosion densities of L415 steel were 0.031 and 0.061 mA.cm⁻² in solutions 1 and 2 in oxygen-free environment, respectively, which belongs to serious corrosion level. The corrosion rate of L415 steel in solution 2 was twice than that in solution 1 environment. Hence, the high salt concentration of the leaching liquid environment caused severe corrosion [19].

Fig.3 shows EIS of L415 pipeline steel obtained in solution 1 and 2. The Nyquist plot in the EIS of L415 steel was roughly the same in solution 1 and 2, with both having one capacitive reactance arc. The low-frequency part of the capacitive reactance arc left skewing and had real component shrinkage, which showed inductive arc feature. Fig. 4 shows the fitting circuit model where R_s represents the resistance, Q_{dl} represents the constant phase angle element reacting to the electric double

layer capacitor, R_{ct} shows the charge transfer resistance, L_{abs} is the inductive reactance for adsorption and R_{abs} is resistance from adsorption layer. The table.4 shows the value of R_{ct} and R_L . The value of R_{ct} decreased when ions increased, which indicated the promoted of L415 steel corrosion from the enhancement of ions. In comparison with the EIS of L415 steel in oxygen-free and oxygen-rich environment, R_{ct} decreased significantly only when oxygen existed under high pressures indicating that oxygen-rich environment accelerated the corrosion of L415 steel.

3.2 Immersion test

3.2.1 Macro morphology

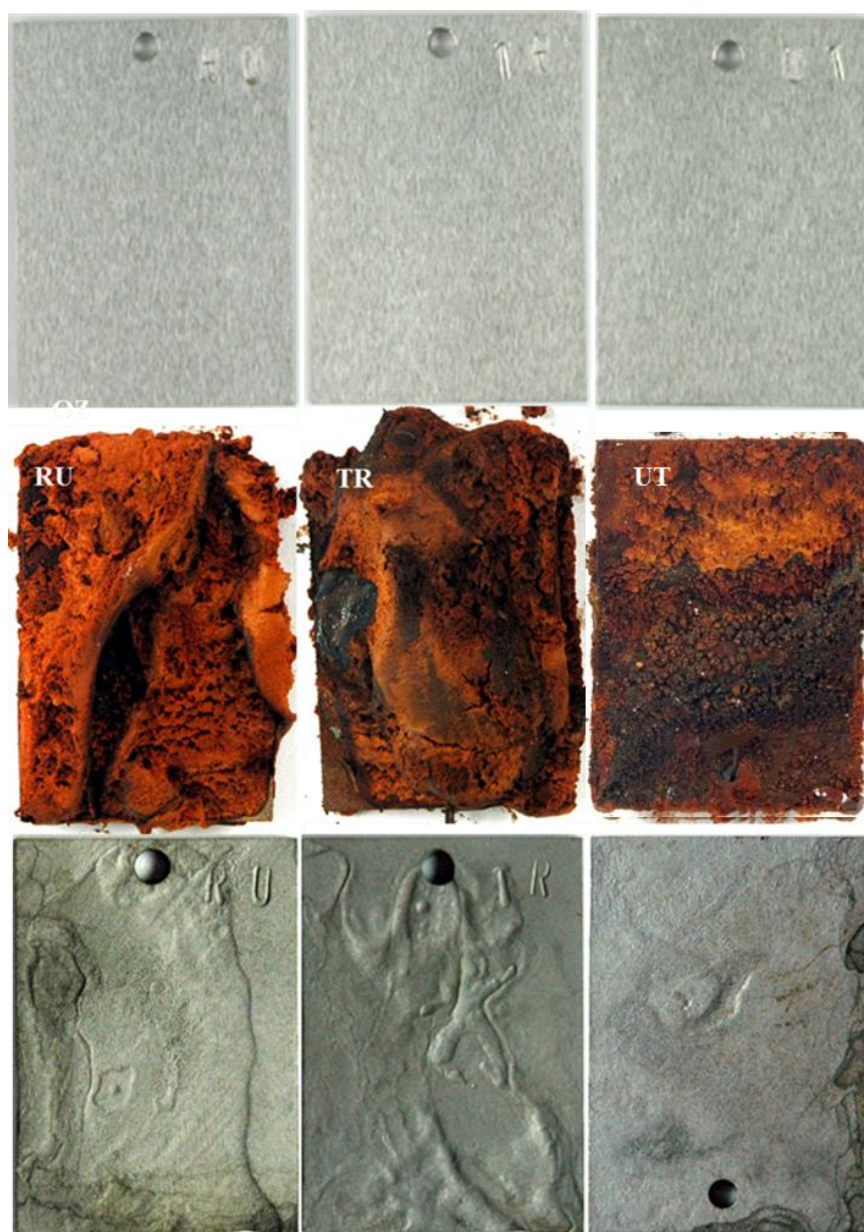


Figure 5. Macro morphology of L415 steel immersed in solution 1 (RU), solution 2 (TR) and solution 3 (UT) with 5MPa 80%N₂-20%O₂ for 90d

Fig.5 shows macromorphology of L415 pipeline steel immersed in solution 1, 2 and 3 for 90d. The sample of RU was in solution 1, TR was in solution 2 and UT was in solution 3. Each environment had three parallel samples. All samples surface were covered with a thick layer of red brown corrosion products after immersed for 90 days in the leaching liquid. Many corrosion grooves in the surface morphology were visible under the naked eye after removing the corrosion products with a descaling liquid (Fig.5). In a word, the corrosion of L415 steel was severe in this high-pressure oxygen-rich and high salt environment.

3.2.2 Micro morphology

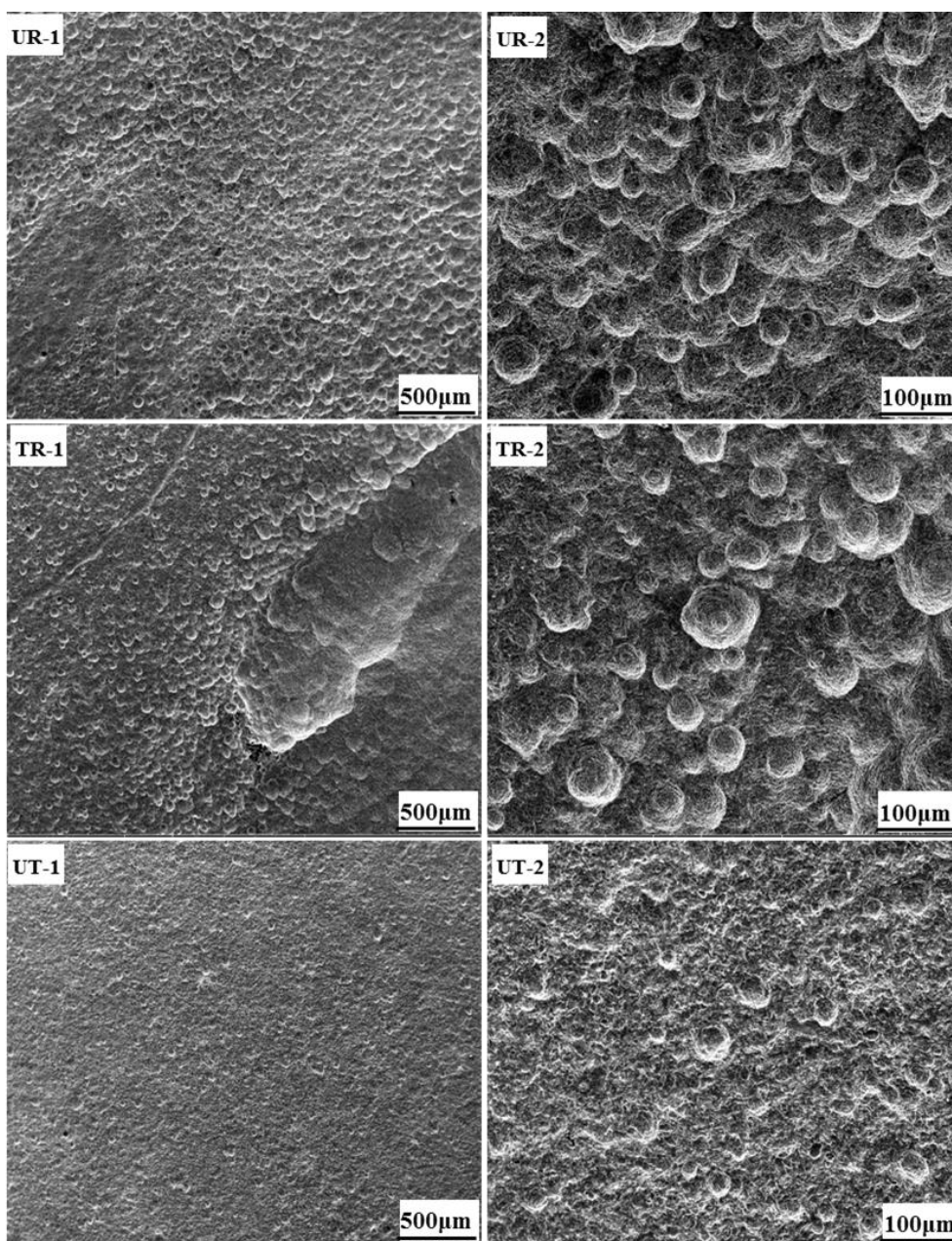


Figure 6. Microstructure of L415 steel immersed in solution 1, 2 and 3 with 5MPa 80%N₂-20%O₂ for 90 days

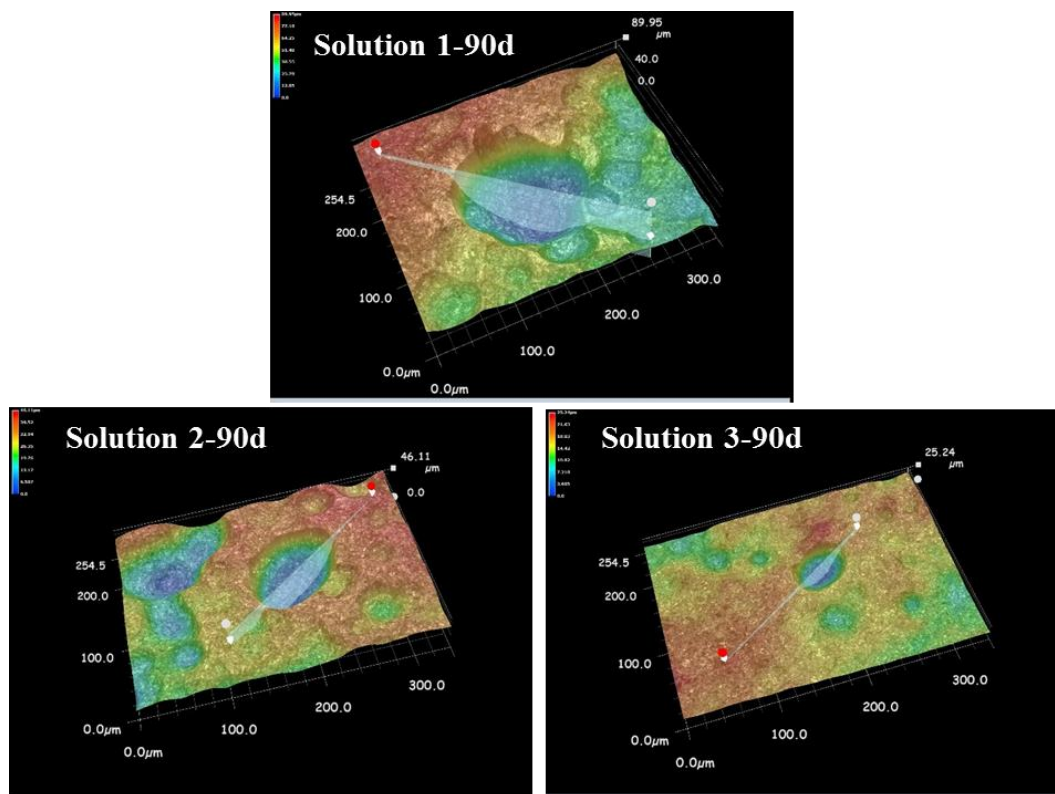


Figure 7. Stereoscopic microscope view of L415 pipeline steel immersed in solution 1, 2 and 3 with 5MPa 80%N₂-20%O₂ for 90 days

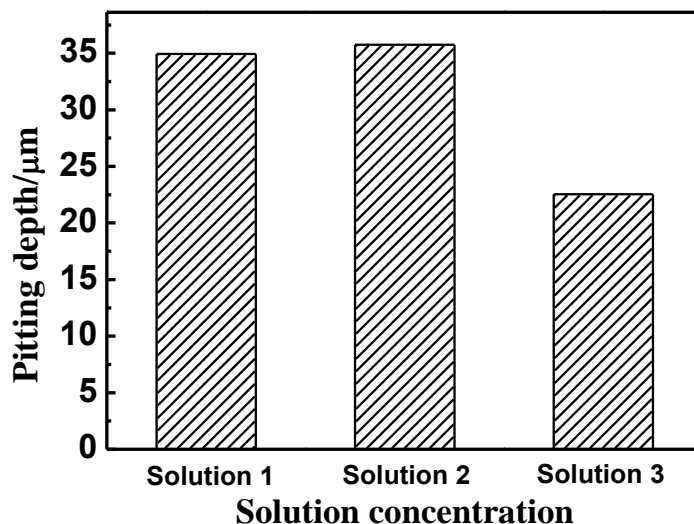


Figure 8. The average maximum pitting depth statistics of L415 pipeline steel immersed in solution 1, 2 and 3 with 5MPa 80%N₂-20%O₂ for 90 days

Fig.6 shows the microstructure of L415 steel immersed in in solution1, 2 and 3 with 5MPa 80%N₂-20%O₂ for 90 days. The sample of RU was in solution 1, TR was in solution 2 and UT was in solution 3. L415 steel generated severe pitting corrosion in solution 1 after immersing for 90 days and the pitting distributed the entire surface of the sample. The surface of the specimen in solution 2

generated severe corrosion groove, and the pitting also distributed the whole sample surface. However, solution 3 brought less pitting, and the depth of pitting was shallow, indicating the uniform corrosion of L415 steel. According to immersion test results, the corrosion of L415 steel was very severe in solution 1. The high salinity of leaching liquid was the major cause of severe corrosion, that is, the salt from sweeping water was the mainly effect for the pitting corrosion of L415 steel.

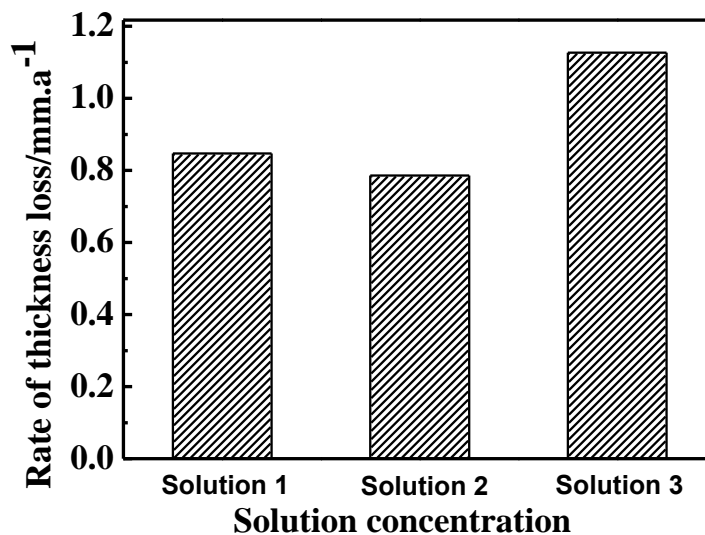
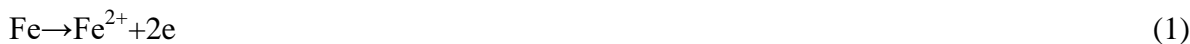


Figure 9. Corrosion rate of L415 pipeline steel immersed in in solution 1, 2 and 3 with 5MPa 80%N₂-20%O₂ for 90 days

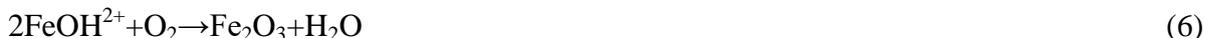
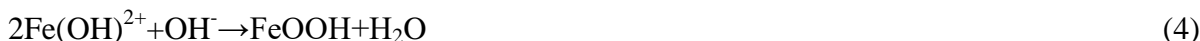
Fig.7 shows the pitting depth of L415 steel immersed in solution 1, 2 and 3 with 5MPa 80%N₂-20%O₂ for 90 days under a stereoscopic microscope. Fig.8 and Fig.9 show average maximum pitting depth statistics and thickness loss rate of L415 steel pipeline immersed in solution 1, 2 and 3 with 5MPa 80%N₂-20%O₂ for 90d, respectively. The pitting depth of L415 steel immersing in solution 1 and 2 was approximately equal, while the depth in solution 3 was shallow. However, the corrosion rate of L415 steel in solution 3 was largest based from the results of Fig. 8. The ions in solution 3 was possibly non-conductive to the growth of the pitting, and the corrosion of sample surfaces occurred uniformly.

3.3 XRD corrosion products analysis

To determine the identity of corrosion products of L415 steel in simulated high-pressure oxygen-rich and high salt environment, corrosion products scraped from the surface of L415 steel were analyzed by X-ray diffraction (XRD) after grinding. Fig 10 shows the results of XRD analysis where the corrosion products were mainly FeOOH, Fe₃O₄ and Fe₂O₃. The mainly reactions were [20,21]:



Given the simulated leaching liquid was an oxygen-rich environment, Fe^{2+} and FeOH^+ dissolved by oxidation [21]:



At the beginning of the corrosion stage, anodic dissolution of Fe occur constantly. The concentration of Fe^{2+} in reaction interface was higher. Therefore, a loose and porous corrosion product layer of FeOOH membrane formed on the electrode surface in a relatively short period of time, corrosion products of Fe_3O_4 and Fe_2O_3 easily form in oxygen-rich environment. Forming the local activation point in space is easy. Because the leaching liquid contains much Cl^- and SO_4^{2-} , Cl^- and SO_4^{2-} would more easily enrich to anode activation nearby through these gap enrichments. The corrosion rate of the electrode increases, then pitting forms [22,23], which results in a local Cl^- gathering in the membrane and the destruction in the dynamic balance of the corrosion product film, then the corrosion of L415 steel occurred in simulated leaching liquid.

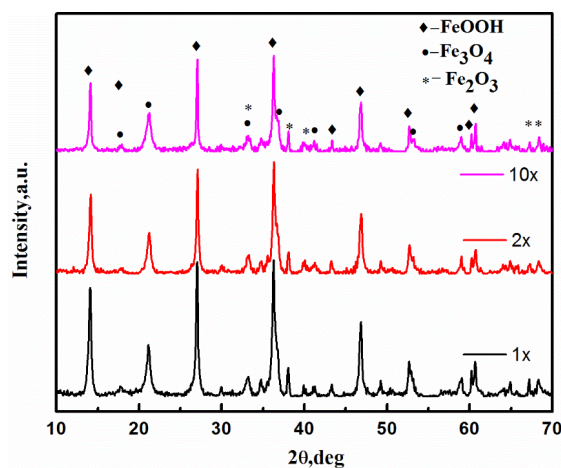


Figure 10. XRD pattern of the corrosion product layer on L415 pipeline steel after 90d immersion in solution 1, 2 and 3 with 5MPa 80% N_2 -20% O_2

4. CONCLUSION

The severe corrosion of L415 steel arises from the high-pressure oxygen-rich and high salt environment. The level of corrosion of L415 steel in this environment is severe with corrosion current density of $0.031 \text{ mA}\cdot\text{cm}^{-2}$ and corrosion rate of $0.847 \text{ mm}\cdot\text{a}^{-1}$. Both leaching liquid ions and oxygen-enriched can promote the corrosion of L415 steel.

In terms of morphology, the L415 steel surface generated a thick layer of corrosion product, the pitting distributed the whole surface; and some areas even had severe corrosion grooves after the removal of corrosion products. Given the severity of L415 steel corrosion, the pipeline should be held under inert atmosphere and swept with water having low salt concentration.

ACKNOWLEDGMENTS

This work was supported by the National Basic Research Program of China (973 Program) (No. 2014CB643300), Chinese National Science Foundation (No. 51471034 and No. 51371036) and Beijing Higher Education Young Elite Teacher Project.

References

1. B. He, P. Han, C. Lu and X. Bai, *Eng. Fail. Anal.*, 58 (2015) 19.
2. J. L. Pacheco, W. J. Sisak, S. Venaik, R. V. Reddy, D. R. Robson, A. Dhokte, E. J. Wright, D. Pugh, C. E. Curtis and S. R. Hickman, *Int. Petr. Technol. Conf.*, International Petroleum Technology Conference, 2007.
3. O. Shabarchin and S. Tesfamariam, *J. Loss.Prevent. Proc. Indust.*, 40 (2016) 479.
4. S. R. Allahkaram, M. Isakhani-Zakaria, M. Derakhshani, M. Samadian, H. Sharifi-Rasaey and A. Razmjoo, *J. Nat. Gas. Sci. Eng.*, 26 (2015) 453.
5. M. Li and Y. Cheng, *Electrochim. Acta*, 53 (2008) 2831.
6. D. Hardie, E. Charles and A. Lopez, *Corros. Sci*, 48 (2006) 4378.
7. L. Shi, C. Wang and C. Zou, *Eng. Fail. Anal.*, 36 (2014) 372.
8. R. K. Stanley, in *IADC/SPE drilling conference*, Society of Petroleum Engineers, 1998.
9. A. R. Crabtree, in *SPE/ICoTA Coiled Tubing and Well Intervention Conference and Exhibition*, Society of Petroleum Engineers, 2008.
10. Y. Hua, R. Barker and A. Neville, *Corrosion*, 71 (2014) 667.
11. B. Yu, D. Li and A. Grondin, *Wear*, 302 (2013) 1609.
12. L. Yucheng, Z. Yinlong, Y. Jianmei, Y. Mengjing and X. Junzhong, *Eng. Fail. Anal.*, 34 (2013) 35.
13. H. X. Wan, X. J. Yang, Z. Y. Liu, D. D. Song, C. W. Du and X. G. Li, *J. Mater. Eng. Perform.*, 26 (2016) 1.
14. A. Rajabipour and R. E. Melchers, *international journal of hydrogen energy*, 40 (2015) 9388.
15. L. Yu, R. François, V. H. Dang, V. L'Hostis and R. Gagné, *Constr. Build. Mater.*, 95 (2015) 384.
16. G. Van Boven, W. Chen, R. Rogge and R. Sutherby, *Acta. mater*, 55 (2007) 29.
17. A. Turnbull, S. Zhou and G. Hinds, *Corros. Sci*, 46 (2004) 193.
18. M. Mohtadi-Bonab, J. Szpunar, R. Basu and M. Eskandari, *Int. J. Hydrogen. Energ*, 40 (2015) 1096.
19. S. Sharifi-Asl, F. X. Mao, P. Lu, B. Kursten, D.D Macdonald, *Corros. Sci*, 98 (2015) 708.
20. J.C. Velázquez, J.C. Cruz-Ramirez, A. Valor, V. Venegas, F. Caleyó, J.M. Hallen, *Eng. Fail. Anal.*, 79 (2017) 216.
21. Z.Y. Liu, Q. Li, Z.Y. Cui, W. Wu, Z. Li, C.W. Du, b, X.G. Li, *Constr. Build. Mater.*, 148 (2017) 131.
22. M.C.Li, H.C.Lin, C.N.Cao, *J. Chine. Soc. Corros. Pro.*, 20(2000)111
23. M. Jafarian, F. Gobal, I. Danaee, R. Biabani, M. Mahjani, *Electrochim. Acta*, 53(2008)4528